Electronic Supplementary Materials

For https://doi.org/10.1631/jzus.A2300436

Influence of vibration on the lubrication effect of a splash-lubricated gearbox

Yi LIU, Kailin ZHANG✉, Shuai SHAO✉, Hongxu XIANG, Zhijian YE

State Key Laboratory of Rail Transit Vehicle System, Southwest Jiaotong University, Chengdu 610031, China

✉ Kailin ZHANG, kailinzhang_swjtu@126.com
Shuai SHAO, swjtushaoshuai@163.com

(Note: In the Electronic Supplementary Materials, a portion of the content is non-core content, formulas, an images, etc., from the manuscript. This part of the content will not be repeated in the manuscript (**marked in blue**). The other part is the content that has appeared in the manuscript, and to maintain the consistency and completeness of the Electronic Supplementary Materials, the complete paragraphs in the manuscript have been moved here.)

Section S1

2.2 Mesh

The numerical model is meshed in the commercial CFD software Simerics-MP +. It uses a unique geometry Conformal Adaptative Binary-tree (CAB) algorithm, which generates Dikar hexahedral meshes in the fluid domain consisting of closed surfaces that are better suited for high-precision algorithms. Close to geometric boundaries, the CAB algorithm automatically adapts the mesh to the geometric surface and geometric boundary lines. To accommodate critical or complex geometric features, CAB automatically resizes the mesh by continuously splitting the mesh, and also automatically increases the mesh density to better resolve geometric features, which is the most efficient way to resolve detailed features using the smallest mesh. Also, some CAD surfaces do not fit perfectly. They may have small gaps, or they may not be specifically sewn together. If the geometry contains such “bad” features, many mesh generation algorithms will fail. Therefore, the geometry must be carefully pre-processed before the mesh is generated. CAB algorithms are somewhat tolerant of “bad” geometries. For the most part, CAB can generate reasonable meshes based on “bad” geometry with negligible loss of accuracy, resulting in meaningful simulation results.

2.3 Boundary condition

Fig. 5(b) shows the time-domain distribution of the vibration acceleration of the gearbox in three directions. As can be seen from the figure, from a peak value perspective, the vibration acceleration of the gearbox can be classified into three regions: Specifically, zone A and zone D pertain to the low-amplitude region, characterized by minor vibration acceleration. zone B belongs to the medium-amplitude region, where the vibration acceleration is primarily small throughout the area. Lastly, zone C pertains to the high-amplitude region, which experiences an uneven section of the track causing noticeably increased vibration acceleration.

The amplitudes of zone A and zone D is too low, and the vibration acceleration in three directions is close to 0, which is not meaningful for the study. The amplitude of transverse vibration in zone C reaches up to 35g, which means that the vehicle encounters a large impact on the track, which is infrequent in the process of vehicle operation and is not universal. In this study, the largest possible amplitude is selected within the normal track upset load range. Obviously, zone B meets the requirements. Therefore, the time-domain distribution of vibration acceleration in three directions within 2.0s of it is selected as the motion boundary condition in this study.

Section S2

2.4.1 Governing equation

Navier-Stokes equations describe the conservation of mass, momentum, and energy as a fluid flows through a three-dimensional system. Since the influence of the thermal effect can be ignored in the simulation process of the incompressible flow field in the gearbox, it is only necessary to satisfy the continuity equation and momentum equation (Deng et al., 2020).

$$\frac{D\rho}{Dt} = 0 \tag{S1}$$

$$\begin{aligned}
\frac{\partial \rho u}{\partial t} + div(\rho u \boldsymbol{u}) &= -\frac{\partial p}{\partial x} + \frac{\partial \tau_{xx}}{\partial x} + \frac{\partial \tau_{yx}}{\partial y} + \frac{\partial \tau_{zx}}{\partial z} + F_x \\
\frac{\partial \rho v}{\partial t} + div(\rho v \boldsymbol{u}) &= -\frac{\partial p}{\partial y} + \frac{\partial \tau_{xy}}{\partial x} + \frac{\partial \tau_{yy}}{\partial y} + \frac{\partial \tau_{zy}}{\partial z} + F_y \\
\frac{\partial \rho w}{\partial t} + div(\rho w \boldsymbol{u}) &= -\frac{\partial p}{\partial z} + \frac{\partial \tau_{xz}}{\partial x} + \frac{\partial \tau_{yz}}{\partial y} + \frac{\partial \tau_{zz}}{\partial z} + F_z
\end{aligned} \tag{S2}$$

$$\begin{cases}
\tau_{xx} = 2\mu \dfrac{\partial u}{\partial x} + \lambda div \boldsymbol{u} \\
\tau_{yy} = 2\mu \dfrac{\partial v}{\partial y} + \lambda div \boldsymbol{u} \\
\tau_{zz} = 2\mu \dfrac{\partial \omega}{\partial z} + \lambda div \boldsymbol{u} \\
\tau_{xy} = \tau_{yx} = \mu(\dfrac{\partial u}{\partial y} + \dfrac{\partial v}{\partial x}) \\
\tau_{xz} = \tau_{xx} = \mu(\dfrac{\partial u}{\partial z} + \dfrac{\partial v}{\partial x}) \\
\tau_{zy} = \tau_{yz} = \mu(\dfrac{\partial v}{\partial z} + \dfrac{\partial w}{\partial y})
\end{cases} \tag{S3}$$

where $\frac{D}{Dt}$ represents the Lagrange time derivative; ρ represents fluid density; u, v, w are the components of the fluid velocity vector $\boldsymbol{u}$; τ_{xx}, τ_{yy}, τ_{zz}, τ_{xy}, τ_{xz}, τ_{zy}, etc are the components of the viscous force acting on the surface of the microelement due to the molecular viscosity action. F_i represents the volume force acting on the fluid element ($i = x, y, z$); p is the pressure on the fluid element; μ is kinematic viscosity.

2.4.2 Turbulence model

The turbulent motion of the oil in a splash-lubricated gearbox is full of randomness (Mastrone and Concli, 2021b) and is characterised by high strain rates and a large degree of streamline bending. This places high demands on the mathematical equations describing the turbulent motion and the meshing of the gearbox model. Reynolds statistically averaged the random effects of turbulence to produce the Reynolds-averaged Navier-Stokes equations (RANS), and addressed this problem with computational precision. Turbulence modelling will reduce computing needs. In studies related to oil flow inside gearboxes, the RNG *k*-*ε* or standard *k*-*ε* model is usually used (Yakhot, et al., 1992). However, the gear meshing region will have strong separation flow and vortex, etc., and the RNG *k*-*ε* model considering turbulent vortex has better computational accuracy for this complex flow. Therefore, the renormalization group (RNG) *k*-*ε* model is used in this paper.

$$\frac{\partial(\rho k)}{\partial t}+\frac{\partial(\rho k u_i)}{\partial x_i}=\frac{\partial}{\partial x_j}[\alpha_k \mu_{eff}\frac{\partial k}{\partial x_j}]+G_k+G_b-\rho\varepsilon-Y_M+S_k \quad \text{(S4)}$$

$$\frac{\partial(\rho \varepsilon)}{\partial t}+\frac{\partial(\rho \varepsilon u_i)}{\partial x_i}=\frac{\partial}{\partial x_j}[\alpha_\varepsilon \mu_{eff}\frac{\partial \varepsilon}{\partial x_j}]+C_{1\varepsilon}\frac{\varepsilon}{k}[(G_k+C_{3\varepsilon}G_b)]-C_{2\varepsilon}\rho\frac{\varepsilon^2}{k}-R_\varepsilon+S_\varepsilon \quad \text{(S5)}$$

Among them

$$\mu_{eff}=\mu+\mu_t, \mu_t=\rho C_\mu \frac{k^2}{\varepsilon} \quad \text{(S6)}$$

where, k is the turbulent kinetic energy and ε is the turbulent dissipation rate. G_k is the turbulent kinetic energy caused by the average velocity gradient. G_b is the turbulent kinetic energy caused by buoyancy. Y_M is the pulsating expansion of compressible fluid; α_k and α_ε are the reciprocal of the effective Prandtl number of k and ε, respectively. μ_{eff} is the effective viscosity; μ is the hydrodynamic viscosity coefficient and μ_t is the turbulent viscosity. S_k and S_ε are the source phases. R_ε appends terms to the model. Where $\alpha_k, \alpha_\varepsilon$, S_k , S_ε, R_ε are all constants in the commercial CFD software Simerics-MP.

2.4.3 VOF Method

There are only two phases, oil and gas, in splash-lubricated gearboxes. To precisely map the oil distribution within the oil-gas combination, the internal flow of the gearbox is evaluated using the VOF two-phase flow model. The VOF model (Hirt and Nichols, 1981) determines the phase interfaces by resolving the continuity equations for the volume ratio of the oil phase.

$$\frac{\partial \alpha_{\text{oil}}}{\partial t}+v_{\text{oil}}\cdot\nabla\alpha_{\text{oil}}=\frac{s_{\alpha_{\text{oil}}}}{\rho_{\text{oil}}} \quad \text{(S7)}$$

In addition, the total sum of the volume fractions of each phase within individual control volumes in the VOF model equals 1.

$$\alpha_{\text{oil}}+\alpha_{\text{air}}=1 \quad \text{(S8)}$$

where, α_{oil} is the oil volume fraction, α_{air} is the air volume fraction, $s_{\alpha_{\text{oil}}}$ is the source phase, ρ_{oil} is the oil density, and v_{oil} is the oil velocity.

2.4.4 Numerical fitting of energy loss

In oil-injected lubricated gearboxes, the no-load power loss can be classified into three main types: impulse power loss, squeezing power loss in the meshing zone, and wind resistance power

loss (Liu et al., 2019). Wind resistance power loss is negligible at low rotational speeds. Impulse power loss occurs when the injected oil hits the tooth surface of the gear, as shown in Fig. 6(c). The squeezing power loss in the mesh zone occurs when oil is forced radially or axially out of the zone.

$$T_I = C_1 \cdot r_\mathrm{p} \cdot \rho \cdot V_\mathrm{in} \cdot (v_\mathrm{t} \pm v_\mathrm{in}) \tag{S9}$$

$$T_S = 4.12 \cdot C_1 \cdot r_p \cdot \rho \cdot V_\mathrm{in}^{0.75} \cdot v_\mathrm{t}^{1.25} \cdot b^{0.25} \cdot m_\mathrm{n}^{0.25} \cdot \left(\frac{\nu}{\nu_0}\right)^{0.25} \cdot \left(\frac{h_0}{h_{z0}}\right)^{0.5} \tag{S10}$$

where C_1 is the variable coefficient, r_p is the nodal circle radius, mm; V_in is the oil injection volume rate, L/s; v_t is the circumferential speed , m/s; v_in is the injection speed, m/s.

Section S3

3.1 Effect of vibration direction

When the locomotive travels at a constant speed in a straight line, the force of gravity acting on the vehicle is balanced by the support force provided by the track. However, the unevenness of the track, including local track irregularities of both the intersection and descending types, generates a significant transient response in the vehicle, resulting in the production of strong and transient vibrations.

3.2 Influence of transverse excitation on lubrication effect

The churning loss over time is shown in Figs. S1(a) and S1(b) for different injection volume rates. From Fig. S1(a), it can be seen that at the starting moment, when the injected fluid has not yet contacted the gears, the churning moment loss curves under the four injection speeds are almost identical. After about 0.2 s, the injected oil hits the tooth surface, causing additional energy loss, and the curves start to diverge. The larger the injection volume rate, the greater the energy loss. Due to the impulse power loss caused by the sprayed oil on the tooth surface, the larger the oil spraying speed, the more energy loss is caused when it impacts the tooth surface. However, compared with the churning loss, the additional loss caused by oil injection lubrication is very small.

As can be seen in Fig. S1(b), the average value of churning moment loss of the gear pair at different injection volume rates is higher than that of the static simulation for the lateral excitation used. Among them, the average value of churning loss for the vibration case at an injection volume rate of 12 L/min is 327% higher than that of the static simulation, which is the largest value of growth rate.

Fig. S2 demonstrates the distribution of the oil volume fraction in the oil-air mixture and the distribution of the velocity trace of the injected oil. As can be seen in Fig. S2, the increase in oil injection lubrication also leads to an increase in lubrication in the bearing region. The oil is ejected from the oil injection holes and shot into the meshing area, and the oil concentration in the upper space in the gearbox increases. The amount of oil entering the bearing oil inlet holes increases. Considering Figs. S3(a) and S3(b) together, it can be seen that with the increase in oil injection speed, the oil supply for the bearings with real-time lubrication efficiency also increases. Among them, the oil supply volume and real-time lubrication efficiency of the GM-side bearing peaked at the oil injection rate of 12 L/min, which were 37.34 g/s and 57.01%, respectively. The oil supply and real-time lubrication efficiency of the GW-side bearing are the smallest when the oil injection rate is 0 L/min, with 7.12 g/s and 18.12%, respectively.

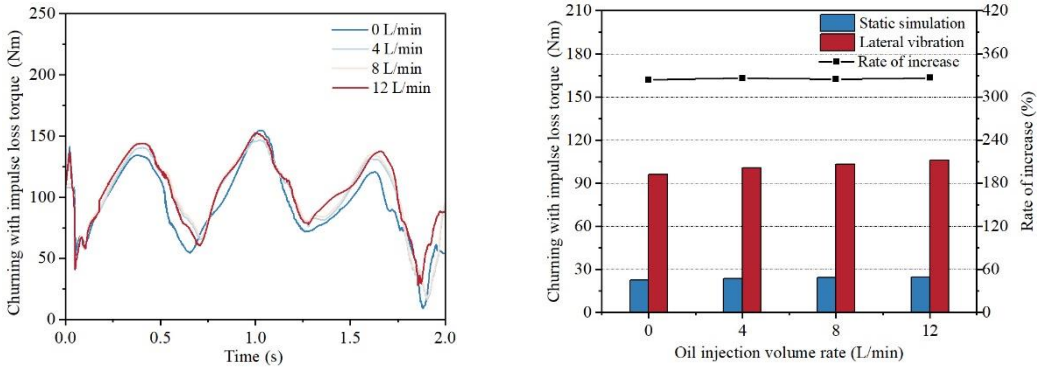

(a) (b)

Fig. S1 Loss of churing with impulse moment under different injection volume rate. ((a) Time-history curve; (b) Comparison of mean value of churing with impulse moment loss in different states)

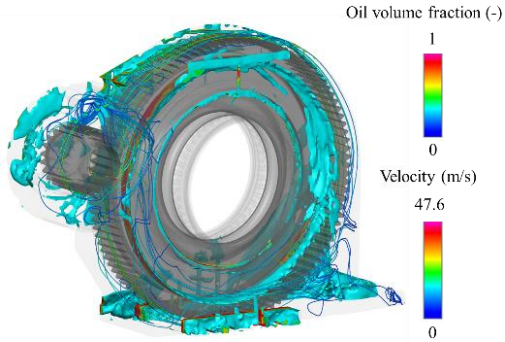

Fig. S2 The flow field of gearbox splash lubrication with jet lubrication.

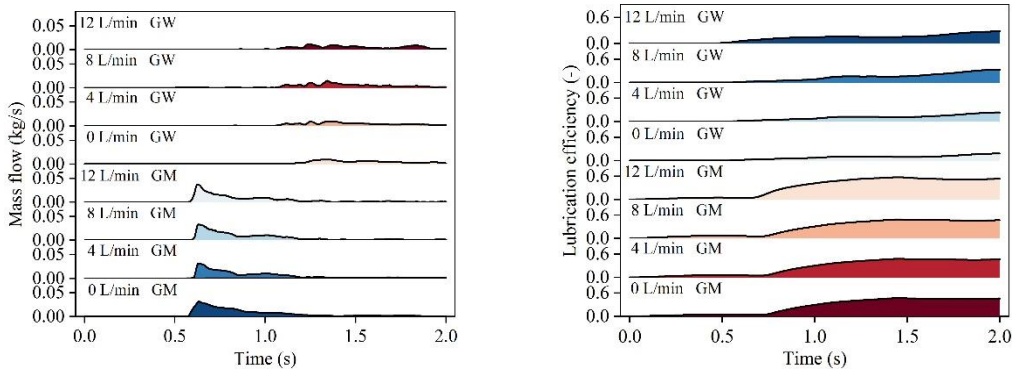

(a) (b)

Fig. S3 The bearings lubrication under different injection volume rate. ((a) Mass flow; (b) Efficiency)

3.3 Comprehensive evaluation of lubrication and efficiency

To comprehensively analyze the lubrication performance and efficiency of the gearbox, three main aspects are evaluated: effective lubrication in critical areas, sealing system performance (Shao *et al.*, 2023) and energy loss. Critical area lubrication can be evaluated by the oil supply for each bearing, the lubrication efficiency and the oil concentration of the end face of the gears; sealing system performance depends on the effective oil concentration and the pressure in the bearing area; and energy loss can be judged by the churning loss. Considering the role of the operational factors, a comprehensive assessment of the gearbox performance, to obtain the

appropriate gearbox operation speed level, the optimal oil quantity and the oil injection volume rate.

The lubrication performance of each condition is obtained by summing the 6 dimensionless numbers under each condition, as shown in Fig. 19. From Figs. 19(a) and 19(b), it can be seen that under the condition of rotational speed of 1600 rpm with immersion depth of 2.0 h, the sum of the 6 dimensionless lubrication evaluation indices is the largest, which is 3.14 and 3.58 respectively, and the comprehensive lubrication performance of the gearbox is the best. For the conditions with oil injection holes, it can be seen that the one hand of the sprayed oil can promote the lubrication performance of the key areas of the gearbox, and the greater the volume rate of oil injection, the greater the lubrication performance improvement; but on the other hand, it makes the transmission efficiency and sealing performance deterioration. In practice, whether to use oil injection lubrication also needs to consider the speed, the degree of difficulty of the installation of the injection system, the cost and other practical issues. Therefore, either only splash lubrication is used, or the largest possible injection volume rate is selected within the appropriate range.